

Continuum x-ray emission spectra from laser-produced plasmas at 10^{16} W/cm 2 [†]

P. G. Burkhalter, F. C. Young, B. H. Ripin, J. M. McMahon, S. E. Bodner, R. R. Whitlock, and D. J. Nagel

Naval Research Laboratory, Washington, D.C. 20375

(Received 19 April 1976; revised manuscript received 29 November 1976)

CH $_2$ and Al targets were irradiated at 10^{16} W/cm 2 with a focused Nd:glass laser to study the dependence of x-ray emission on laser-pulse parameters. Complementary optical diagnostics indicated that 60–80% of the incident laser energy was absorbed in the planar targets. X-ray intensities spanning eight orders of magnitude were measured from 1 to above 100 keV by the multiple absorption foil method. The spectral shapes for CH $_2$ targets were independent of pulse length for 21- and 250-psec pulses.

I. INTRODUCTION

Measurements of absolute x-ray emissions from laser-produced plasmas can provide important insight into the physics of plasma heating. Impetus for the work reported here stemmed from the lack of agreement between measured x-ray emission¹ from plasmas irradiated with 25-psec pulses of approximately 10^{16} W/cm 2 and numerical code predictions.² The computer code incorporated a so-called superthermal electron distribution, within a hydrodynamic framework of plasma expansion, to simulate experimental x-ray emission spectra. The x-ray measurements in this work were from solid CH $_2$ targets at a laser irradiance of $\sim 10^{16}$ W/cm 2 with 1.06- μ m laser light. Laser pulse durations of 21 and 250 psec, FWHM, were used. The x-ray absorption filter method was chosen so as to cover a broader energy range than was previously reported¹ (i.e., from 1 to above 100 keV). This allowed both the low-energy and higher-energy bremsstrahlung distributions to be measured simultaneously.

The bremsstrahlung spectrum was measured at a longer pulse length of 250 psec to determine the spectral shape of the x-ray emission at a pulse length closer to that being considered for fusion pellet design.³ In this case the electron-electron collision time is short compared with the heating time and the hydrodynamic approximation is better satisfied. The shape of the x-ray spectral distribution from CH $_2$ was found to be independent of the laser pulse length. X-ray emission was also measured for an Al target at 250 psec because moderately heavy elements are being used as outer coatings or as glass shells to achieve compression of the lower atomic number interior in laser fusion pellets.

We performed careful measurements of the laser beam characteristics and focal conditions, and determined the amount of laser light absorbed by the slab CH $_2$ targets. These laser parameters are important in the understanding of the physics of the

x-ray emission and would be required for meaningful calculations of the bremsstrahlung spectral distribution using hydrodynamic computer codes.

II. EXPERIMENTAL

A. Laser and target properties

The Naval Research Laboratory (NRL) Nd:glass laser ($\lambda_0 = 1.06$ μ m) was operated above 4×10^{10} W to irradiate slab targets at normal incidence in an evacuated ($\sim 10^{-4}$ Torr) chamber. Both x-ray and plasma measurements were made using 21 ± 2 psec and 250 ± 25 psec pulses focused with a $f/1.9$ aspheric lens onto 0.75-mm thick polyethylene planar targets of 99.999% purity. The Al targets were 99% pure.

B. Focal position determination

The lens-target focal position was determined by monitoring the intensity of energetic x rays (~ 20 keV) as a function of the distance between the target surface and the lens. Before making spectral measurements, a series of shots was taken to locate the target focal position as determined by the intensity of x rays. Best focus was assumed coincident with the maximum x-ray intensity. An offset from focus of 200 μ m decreased this x-ray signal by a factor of 2. At best focus as determined in this manner, spherical craters were produced in the target surface by the laser-target interaction.

After the optimum target position was determined, the focal intensity distribution in the target plane was measured. One method involved measuring the diameter of the burn patterns formed by ablation of thin (~ 200 Å) bismuth films from glass plates. The ablations were performed with the laser beam attenuated by varying known amounts. The results were confirmed independently by firing the laser at full power through a pinhole placed at focus with a calorimeter monitoring the transmitted energy. The laser focal spot intensity distribution

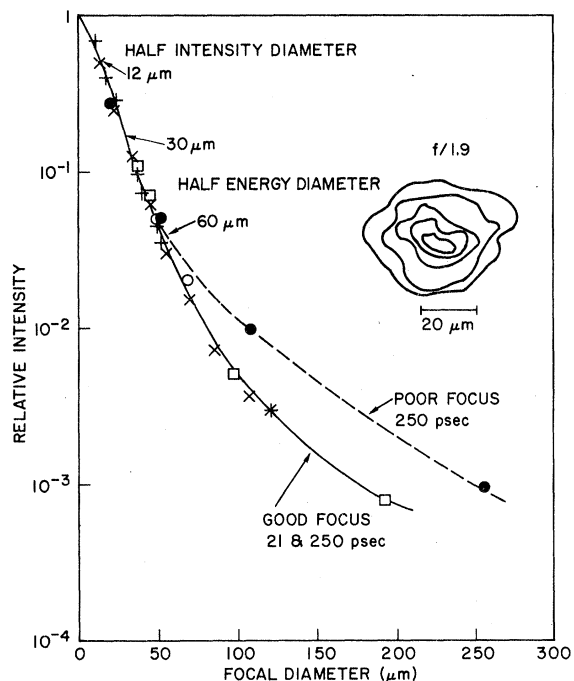


FIG. 1. Laser focal spot intensity vs diameter for 21- and 250-psec pulse durations. Thin film ablation data were taken for 21-psec pulses with attenuated $\sim 10^7$ -W shots (+), $\sim 10^{11}$ -W shots (\square), and, respectively, for 250-psec pulses (\times , \circ) at good focus and (\bullet) at poor focus. The point denoted by (*) was obtained by measuring the fraction of the beam's energy passing through a 120- μ m diameter pinhole placed at focus.

is plotted vs the mean ablation area diameter in Fig. 1 for both 21- and 250-psec laser-pulse lengths. The half-intensity diameter of 12 μ m was thus obtained from the intensity distribution shown in Fig. 1. The energy contained within a given diameter at focus is obtained by integrating the intensity distribution over area. From these distributions it was determined that half of the laser energy was deposited in a 30- μ m-diameter spot for all the 21-psec pulses and for the majority of the reported 250-psec data. Some data were also collected at 250 psec with a half-energy focal diameter of 60 μ m (see Fig. 1).

C. Laser energy absorption

In order to evaluate the conversion efficiency of incident laser light into x rays, it is necessary to know the amount of laser light that is absorbed by the target. Measurements were made of the scattered light from CH_2 and Al targets to infer the fraction of absorbed energy. Incident and backscattered laser energies were measured with calorimeters viewing beam splitters at near normal incidence. Backscattered light, which is a combination of specular reflection and stimulated

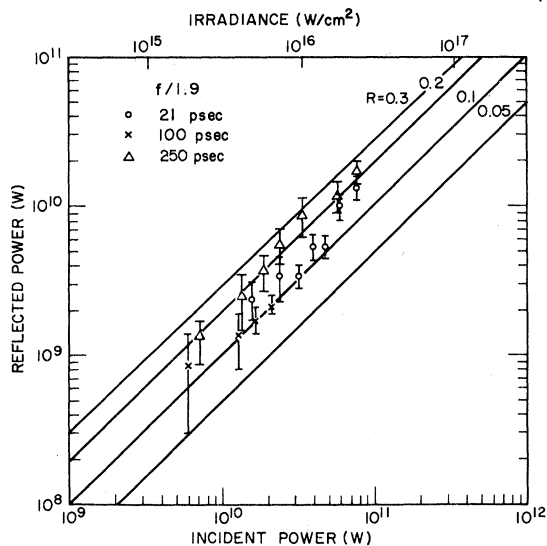


FIG. 2. Backscattered power vs incident power for 21, 100, and 250-psec laser pulses incident on CH_2 targets. A peak incident irradiance scale is provided on the basis of the focal diameters as determined by data in Fig. 1. The symbol R is the fraction of backscattered laser light.

Brillouin backscatter,⁴ is defined as that light scattered back through the focusing lens towards the laser. The back reflection coefficient, shown in Fig. 2, is approximately $15 \pm 5\%$ for laser irradiances in the range of $\sim 10^{15}$ W/cm² to greater than 2×10^{16} W/cm² for laser pulse lengths of 21, 100, and 250 psec. Incident and backreflected pulse shapes and spectra were measured by an ultrafast ($\tau \sim 5$ psec) streak camera focused onto the focal plane of a 2-m Ebert-type spectrograph.

The scattered light falling outside the solid angle of the focusing lens was also measured by wrapping calibrated photocopy paper 360° around the target except for an entrance hole for the incident laser beam. The scattered light detected by the photocopy paper was about 5% of the incident laser beam. Most of this scattered light appeared just outside the lens solid angle. However, since the threshold of the photocopy paper was approximately 30 mJ/cm² for exposure and the area of the exposed surface was about 12 cm², then the fraction of incident laser energy that could remain undetected would be approximately 20%. Therefore, between 60 and 80% of the incident laser energy was absorbed by the CH_2 targets for both 21- and 250-psec pulse durations and for Al at 250-psec pulses.

D. Initial conditions at target surface

Diagnostics were provided which determined the extent of plasma formation at the target surface just prior to the main laser pulse. The presence

of even low-density plasma at the target can possibly change the thermal conductivity at the surface sufficiently to alter the nature of the interaction and hence the x-ray spectrum. There are two Pockels-cell optical gates in the laser. One Pockels cell (No. 1) switches out a single-mode locked pulse from the oscillator pulse train. The other Pockels cell (No. 2), which operates after several amplifier stages, increases the ratio of the switched out laser pulse energy to that of rejected pulses, spurious pulses, and spontaneous emission.

A Jamin interferometer using frequency-doubled 1.06- μm light (5320 Å) as a probing beam parallel to the target surface was used to determine the extent of plasma formation. For most shots the interferogram was taken 0.2 nsec before the main pulse arrived to diagnose the prepulse plasma. The plasma condition at this time would be nearly the same as at the arrival time of the main pulse. With only one Pockels cell operating, sufficient laser energy from a train of leakage pulses (8 pulses were measured with 9-nsec spacings and energies of less than 2 mJ) strikes the target preceding the main pulse to produce a plasma of average density $n_e = 2 \times 10^{18} \text{ cm}^{-3}$ over a 300- μm -diameter volume. No plasma is detected when both Pockels cells are functioning. Indeed, less than 25 μJ of the mode-locked pulse energy strikes the target before the main pulse with both Pockels cells operating.

E. X-ray detectors

Thirteen active detectors were used simultaneously to measure the x-ray spectrum from 1 to above 100 keV. Energy discrimination was achieved using both K edge and broadband x-ray absorption filters.

Five NaI(Tl) detectors, 3.8 cm in diameter, were used to measure high energy x rays (above 30 keV). These detectors were located on individual vacuum chamber ports at 45° to the incident laser-beam direction, i.e., behind the target. High- Z x-ray absorption filters were located 10 cm in front of the NaI(Tl) crystals in order to minimize contributions from fluorescence of the high- Z filters. The thickness of each absorber and NaI(Tl) scintillator was selected to optimize the detector-filter response to x rays just below the K edge of the filter material. Lead collimation was used to shield against x rays produced from possible energetic electron collisions at the chamber walls. To measure moderate x-ray energies from 4 to 30 keV, four NaI(Tl) scintillators, 0.6 cm in diameter, were mounted in an extension pipe at 135° to the laser-beam direction. Both the moderate and high-energy sets of scintillation detectors were calibra-

ted in photon energy with 122-keV gamma radiation from the radioisotope ^{57}Co .

Low energy x rays (below 4 keV) were detected by four PIN Si diodes positioned at 135° to the laser beam. The PIN detectors had 250- μm active thicknesses. The PIN diode sensitivity was calculated based on the response of silicon to x rays using a value of 3.66 eV⁵ per charge pair. The PIN diodes were covered with thin light-tight Be foils. Tests were performed by covering the diodes with glass to insure that spurious signals did not arise from light leakage rather than from x rays.

The range of sensitivities of the various x-ray detectors together with variations in the detector solid angles allowed the collection of the spectral data over eight orders of magnitude. Signals from all detectors were recorded simultaneously on either oscilloscopes or transient recorders. The details of each of the 13 detectors in terms of absorption filter and detector thicknesses, their x-ray energy response, and solid angle are available

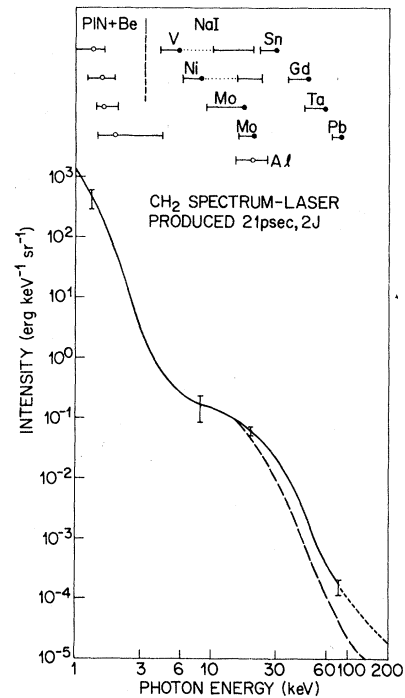


FIG. 3. Average x-ray spectral emission for the 21-psec laser pulse. The energy responses of the x-ray absorption filter-detector combinations are shown above the emission curves. The solid curve represents emission in the 45° (forward) direction while the long dash curve is for emission at 135° to the laser beam direction (see text). The vertical bars on this graph at 1.4, 20, and 85 keV indicate the precision of the measurements while the accuracy has been determined to be a factor of two. Broadband filters are denoted by (○) and K -edge filters by (●).

upon request. The choice of absorption filters used for the 21-psec data are presented at the top of Fig. 3.

III. RESULTS

X-ray signals were collected for a large number of laser shots at focus under known laser conditions. X-ray spectra were extracted from a total of 25 different shots on CH₂ for which signals were measurable on all 13 detectors. Signals from the detectors were computer processed to fit an x-ray spectrum in the following manner. The computer code⁵ was used to calculate the integral response for each detector-filter combination from a trial spectrum. The first trial spectrum was an exponential distribution that varied over the same intensity range as the measured data from the lowest to the highest energy. Computed detector responses were compared with the measured x-ray signals for each detector. Manual adjustments were made to the trial spectrum to bring the calculated detector response into agreement with the measured signals. Iteration of this procedure, usually requiring up to ten runs, was made until no further improvement was obtained. Agreement at the 10–20% level between computed and measured responses was obtained for at least ten of the detectors on each shot. Larger discrepancies between the measured response and the computed spectral distribution were observed for some individual detectors. The reason for these discrepancies is unclear.

The spectrum of x-ray emission for a 2 J, 21-psec laser pulse on a CH₂ target is shown in Fig. 3. The solid line represents the x-ray emission in the 45° (forward) direction assuming isotropy of x-ray emission below 20 keV.^{6,7} Slivinsky *et al.*⁸ recently reported 45°/135° intensity-ratio anisotropy values of 2 at 25 keV and 5 at 100 keV for x rays generated with CD₂ targets and 4-nsec pulse lengths. The dashed curve in Fig.3 for energies higher than 20 keV is the x-ray emission at 135° assuming Slivinsky's anisotropy values are valid for the present experiment. The highest energy K-edge filter in our experiment is Pb at 88 keV. Above 88-keV energy, the spectrum is dashed to indicate uncertainty due to poor photon counting statistics in the highest energy, broadband, Ta filter-detector combination.

Separate experiments were designed to determine the absolute and relative error limits of the x-ray intensity measurements in this work. These absolute and relative error estimates were determined in part by a set of experimental cross checks between the different detection systems used and with calibrated no-screen x-ray film. The absolute

uncertainty of the spectral intensities from 1.2 to 88 keV is estimated to be a factor of 2. The relative error in measuring the x-ray emission for any one laser shot is less than 30% over this energy range.

At 21 psec, x-ray spectra were obtained for incident energies of 0.64–3.3 J at a focal size of 30- μ m diameter at half-energy content. Therefore, the irradiance varied from 4×10^{15} to 2×10^{16} W/cm². X-ray spectra for five different shots at 21 psec are shown in Fig. 4. The individual spectra are identified as to laser shot number and the laser energy on target. The data group with the lower shot numbers in Fig. 4 was collected with only one Pockels cell in operation while the rest of the data in this work were acquired with two Pockels cells. All of the spectra have the same basic shape consisting of a low-temperature component in the 1–3.5-keV energy region and a higher temperature component in the 20–60-keV energy region. Above 60 keV, x-ray bremsstrahlung is more intense than implied by extrapolating these temperature components. Figure 4 exhibits shot-to-shot variations in the spectral emission which will be discussed later.

X-ray spectra obtained with 250-psec laser pulses of 7–12 J incident on a CH₂ target at a focal size of 30- μ m diameter are presented in Fig. 5.

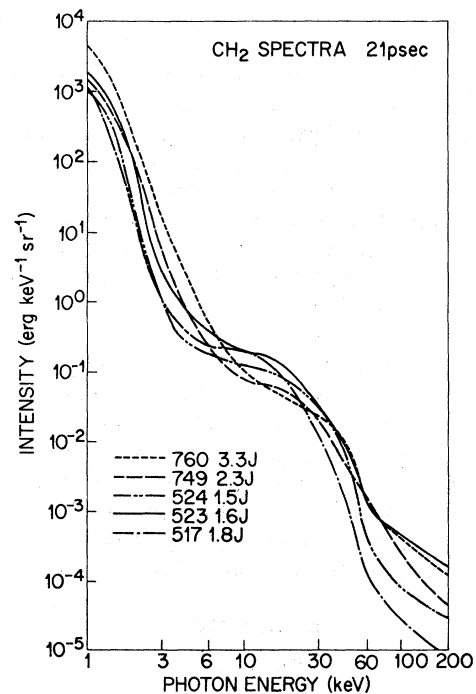


FIG. 4. Individual x-ray spectral emissions for CH₂ at 21 psec (shot numbers and laser energy indicated for each spectrum).

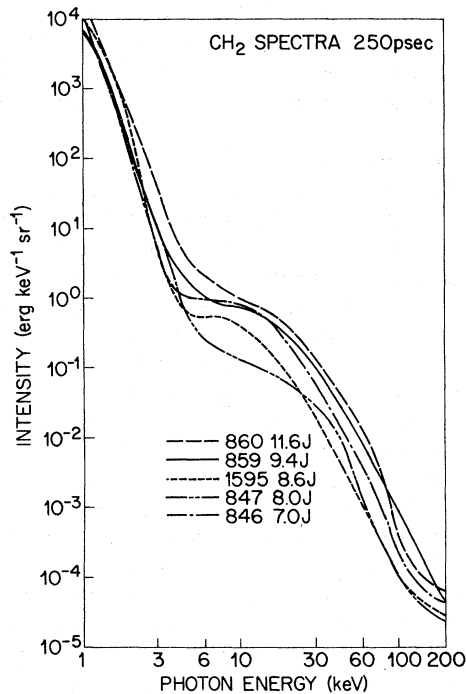


FIG. 5. Individual x-ray spectral emissions for CH_2 at 250 psec.

The irradiance varied from 4 to $7 \times 10^{15} \text{ W/cm}^2$. Both a low-temperature component between 1 and 3.5 keV and higher-temperature components are present. Also the shot-to-shot variation is about the same as the shorter pulse length. An average of the five 250-psec shots is compared with the average 21-psec spectrum in Fig. 6. The shaded areas represent the envelope of spectral data excluding shot 760 at 21 psec. The average spectral curves have the same shape for the two pulse lengths over the entire energy range. The average spectral intensity for the 250-psec data is higher than for 21 psec by about the difference in the incident laser energy.

The spectrum obtained with an Al target for a 250 psec, 6.7-J pulse at an irradiance of $4 \times 10^{15} \text{ W/cm}^2$ is shown in Fig. 7. Most of the continuum radiation from Al occurs above 2 keV , the ionization level for hydrogen-like Al ions. Below 20 keV , the x-ray intensity from Al exceeds that from CH_2 at 250 psec, but at higher energies the emission from these targets is comparable.

IV. DISCUSSION

A. Spectral variations

As can be seen in the x-ray emission data at both laser pulse lengths (Figs. 4 and 5), the variations in the spectral distributions are outside the

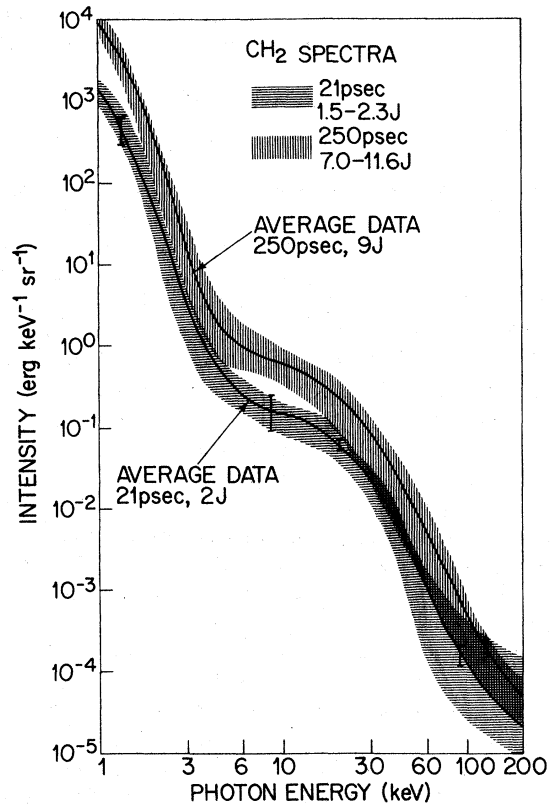


FIG. 6. Comparison of 21- and 250-psec x-ray spectral emission for CH_2 . The crosshatching gives the range of the spectral variations for both pulse lengths.

30% measurement precision. However, good reproducibility of the x-ray spectra within the limits of the shot-to-shot variations were observed for both pulse lengths over the entire x-ray energy range, provided the laser conditions were sufficiently constant and the target was at the proper focal position. Generally the magnitude of the intensity fluctuations from shot-to-shot was the same for all detectors at a given laser energy. On a few shots ($< 10\%$) nearly all the detectors showed an increase in the x-ray emission of as much as an order-of-magnitude. We were unable to correlate laser pulse condition with the occasional shot that produced enhanced x-ray emission. We can rule out the presence of a low-density prepulse condition at the $2 \times 10^{18} \text{ electrons/cm}^3$ level because no significant change in x-ray spectra within the shot-to-shot fluctuations of the spectral envelopes was observed from shots with one or two Pockels cells in operation.

Spectral data were collected to determine the variation in x-ray emission with laser irradiance at a constant laser energy. Several shots including No. 1595 were taken at 250 psec at a lower ir-

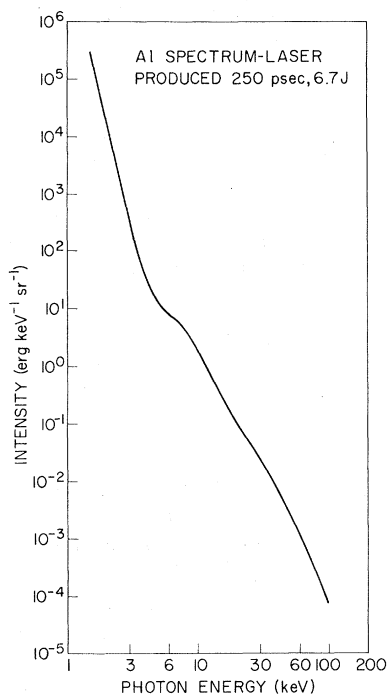


FIG. 7. X-ray spectral emission for Al at 250 psec.

radiance of 1×10^{15} W/cm² by using a 60- μ m diameter focused beam. Under these conditions the intensity of the low-energy portion of the spectrum did not change appreciably but higher-energy (> 20 keV) x-ray emission was reduced by a factor of 2 to 5.

B. Comparison with other experiments

The spectra obtained at 21 psec in the present experiment for CH₂ targets are compared with spectra obtained at the Los Alamos Scientific Laboratory (LASL) at the same irradiance level of 10^{16} W/cm² but at a higher incident laser energy. In order to compare results we need to know the scaling of the x-ray intensity with incident laser pulse parameters. Data have been reported⁹ for the variation in x-ray intensity with incident laser energy for Nd:glass laser pulses on CH₂ targets. The x-ray emission measured at 20 keV scaled roughly as (incident energy)^{2/3} between 5 and 100 joules for both 250 and 900-psec pulse lengths. In the present investigation, the x-ray emission for each detector-filter combination was found to increase at a less than linear rate for both 21 and 250-psec laser pulses. The average rate of increase at 21 psec was (incident energy)^{0.65 ± 0.20} over the range of 0.64–3.3 J. The LASL spectra were normalized to the 2-J level by scaling the x-ray intensities as the two-thirds power of the laser energy. Good agreement was obtained. The

two LASL shots differed from each other by an amount similar to the shot-to-shot variation observed in the NRL measurements.

The x-ray spectral emission from CD₂ targets irradiated by a Nd:glass laser system at 1.6×10^{13} W/cm² with 4-nsec pulse duration has been reported by Slivinsky *et al.* at Lawrence Livermore Laboratory (LLL).⁸ Their measurements were performed by the K-edge filter technique for the energy range of 1–115 keV. The qualitative overall shape of the CD₂ spectral emission is similar to the NRL data. The log-log plot⁸ of the x-ray intensity vs x-ray energy has a sharp break at about 3 keV. In the LLL experiment at lower intensities and longer pulse lengths, the high-energy bremsstrahlung emission is attributed to superthermal electrons.^{2,8}

C. Plasma temperatures

The soft x-ray emission from 1 to about 3.5 keV was found to decrease exponentially with nearly the same slope for each laser shot. Assuming that thermal equilibrium exists in the plasma, Maxwellian electron temperatures of 250 ± 25 and 240 ± 25 eV are determined from the 21- and 250-psec measurements, respectively. These temperatures are sufficient to insure that 97% of the carbon atoms in the plasma are completely stripped of electrons. The low temperature was found to be independent of the laser pulse duration and laser energy at a constant irradiance. The averages of the x-ray spectra at 21 and 250 psec, when replotted on a semilog graph, are nearly linear from 4 to 60 keV with temperatures near 10 keV. On individual shots most of the spectra are nearly linear in the 20–60-keV region with temperatures of 10 ± 5 keV. Temperatures deduced from this higher-energy region did not show any correlation with laser energy at either 21 and 250 psec.

The low-energy thermal component for the Al spectrum has a temperature value of 360 ± 50 eV and the higher energy bremsstrahlung emission for the Al spectrum corresponds to T_e equal to 6 keV; however, the uncertainty in this single-shot determination is unknown.

D. Total x-ray emission

To determine the total x-ray emission, some measurements of the angular distribution were performed. The intensity of x rays near 20 keV was measured by using 1-mm Al filters and NaI(Tl) scintillation detectors positioned at 45° and 135° to the incident laser beam. The x-ray emission was isotropic within the 20% precision of the measurements at these positions for 100-psec laser pulses. This result is consistent with measurements⁹ on

CH₂ for 0.25 and 0.9-nsec laser pulses. Also four scintillation detectors with 1-mm Al filters were used to determine that the x-ray emission near 20 keV was isotropic within 20% over 1% of 4 π solid angle at $\pm 135^\circ$ to the laser beam for 250-psec laser pulses. For lower energy x rays we have assumed angular isotropy based on reported measurements.^{6,7} Above 20 keV, significant anisotropy is indicated by the results of Slivinsky *et al.*⁸

The total x-ray emission from CH₂ plasmas was determined by integrating spectral data for both 21- and 250-psec pulse lengths. The measured x-ray emission between 1–5 keV into 4 π was 0.02% of the incident laser energy on the target. The x-ray emission from 5 to 50 keV was only 1% of that from 1 to 5 keV. These percentages apply to both pulse lengths.

V. SUMMARY AND CONCLUSIONS

The x-ray spectral emissions from CH₂ and Al were measured at a laser irradiance of $\sim 10^{16}$ W/cm² using the multiple absorption-foil method. The 1.06- μ m laser light was focused to 30- μ m diameter

at half energy with an $f/1.9$ lens. At focus, the absorption of the incident laser energy was determined to be 60–80% for planar targets. The presence of a low level (2×10^{18} cm⁻³) preplasma, resulting from leakage prior to arrival of the main mode-locked pulse, had no detectable effect on the x-ray spectra. The spectral shapes were found to be invariant with laser pulse durations of 21 and 250 psec. The x-ray intensity scaling in this work is consistent with two-thirds power of the incident laser energy. Two temperature components were found in the x-ray emission, a 250-eV component from 1 to 3.5-keV photon energy and a 10 ± 5 -keV component up to 60-keV photon energy.

ACKNOWLEDGMENT

The authors are grateful to other people at the Naval Research Laboratory who made valuable contributions to the work being reported in this manuscript. These are L. S. Birks, J. A. Stampfer, D. J. Johnson, C. M. Dozier, R.D. Bleach, and E. A. McLean. The technical assistance of T. DeRieux and E. Turbyfill was appreciated.

†Work performed under the auspices of the United States Energy Research and Development Administration.

¹J. F. Kephart, R. P. Godwin and G. H. McCall, *Appl. Phys. Lett.* **25**, 108 (1974).

²H. D. Shay *et al.*, Superthermal Electron Distributions in Laser-produced Plasmas, UCRL-75465, 1974 (unpublished).

³J. Nuchols, L. Wood, A. Theisen, and G. Zimmerman, *Nature* **239**, 139 (1972).

⁴B. H. Ripin, J. M. McMahon, E. A. McLean, W. M.

Manheimer, and J. A. Stamper, *Phys. Rev. Lett.* **33**, 634 (1974).

⁵D. J. Johnson, *Rev. Sci. Instrum.* **45**, 191 (1974).

⁶K. Eidmann and R. Siegel, in *Proceedings of the Sixth European Conference on Controlled Fusion and Plasma Physics*, Moscow, 1973, p. 435 (unpublished).

⁷C. E. Violet, W. H. Grasberger, J. Petruzzi, and L. M. Richards, *Bull. Am. Phys. Soc.* **20**, 682 (1975).

⁸V. W. Slivinsky, H. N. Kornblum, and H. D. Shay, *J. Appl. Phys.* **46**, 1973 (1975).

⁹F. C. Young, *Phys. Rev. Lett.* **33**, 747 (1974).